Chinese Journal of Chemical Engineering 28 (2020) 2382–2390

Contents lists available at ScienceDirect

Chinese Journal of Chemical Engineering

journal homepage: www.elsevier.com/locate/CJChE

Article

A comparative process simulation study of Ca—Cu looping involving post-combustion CO_2 capture

Xiaoyu Wang, Haibo Zhao *, Mingze Su

State Key Laboratory of Coal Combustion, School of Energy and Power Engineering, Huazhong University of Science and Technology, Wuhan 430074, China

ARTICLE INFO

Article history:
Received 10 May 2020
Received in revised form 11 June 2020
Accepted 23 June 2020
Available online 29 June 2020

Keywords:
Ca—Cu looping
CO_2 capture
Process systems
Numerical simulation
Exergy

ABSTRACT

This work presents a simulation study of several Ca—Cu looping variants with CO_2 capture, aiming at both parameter optimization and exergy analysis of these Ca—Cu looping systems. Three kinds of Ca—Cu looping are considered: 1) carbonation–calcination/reduction–oxidation; 2) carbonation–oxidation–calcination/reduction and 3) carbonation/oxidation–calcination/reduction. A conventional Ca looping is also simulated for comparison. The influences of the calcination temperature on the mole fractions of CO_2 and CaO at the calciner outlet, the $CaCO_3$ flow rate on the carbonator performance and the Cu/Ca ratio on the calciner performance are analyzed. The second kind of Ca—Cu looping has the highest carbonation conversion. At 1×10^5 Pa and 820 °C, complete decomposition of $CaCO_3$ can be achieved in three Ca—Cu looping systems, while the operation condition of 1×10^5 Pa, 840 °C is required for the conventional Ca looping system. Furthermore, the Cu/Ca molar ratio of 5.13–5.19 is required for the Ca—Cu looping. Exergy analyses show that the maximum exergy destruction occurs in the calciner for the four modes and the second Ca—Cu looping system (*i.e.*, carbonation–oxidation–calcination/reduction) performs the highest exergy efficiency, up to 65.04%, which is about 30% higher than that of the conventional Ca looping.

1. Introduction

Electricity generation from the combustion of fossil fuels such as coal contributes more than 30% of total CO_2 emissions, which aggravates the global greenhouse effect. CO_2 capture and storage (CCS) technology for coal-fired power plants is becoming more and more significant and urgent to solve the global warming issues [1]. Currently, lots of researchers are paying attention to the mono-ethanolamine (MEA)-based post-combustion carbon capture technology and the integrated gasification combined cycle (IGCC)-based pre-combustion carbon capture technology and oxy-combustion carbon capture technology [2–4]. However, there are many problems associated with these technologies, such as the degradation of the sorbents in the post-combustion technology and the requirement of a high-cost/high-energy-consuming cryogenic air separation unit (ASU) in the pre-combustion technology and the oxy-combustion technology. The above problems prompt researchers to find out novel CO_2 capture technologies.

As a post-combustion CO_2 capture technology, the carbonation–calcination looping (Ca looping) process was formally proposed by Shimizu *et al.* [5]. In this process, CaO absorbs CO_2 from the flue gas to produce $CaCO_3$ in the carbonator. The generated $CaCO_3$ is then calcined in the calciner to get the high purity CO_2, meanwhile the sorbent CaO is regenerated which can be transferred back to the carbonator for the next cycle. Ca looping has attracted significant interest because of the inexpensive raw materials and high CO_2 capture capacity of the CaO sorbent.

However, the decomposition of $CaCO_3$ is an intensively endothermic reaction and requires a lot of heat which is usually provided by the oxy-combustion of additional fuels. The requirement of high-purity O_2 in the oxy-combustion significantly increases the energy consumption and the operation cost of the overall process. Integrating chemical looping combustion (CLC) with Ca looping can substantially solve the problem as the exothermic oxidation and/or reduction of the oxygen carrier (OC) can provide heat to the decomposition of $CaCO_3$ [6–8]. Generally, the oxidation of OC is an intensively exothermic process, while the reduction of OC is a slightly exothermic process or even an endothermic process, depending on the kind of the OC used. The intuitive idea is to couple the air reactor (AR) in CLC with the calciner in Ca looping, so that the heat requirement in calcination can be satiated by the exothermic oxidation reaction of OC. However, in this case, the CO_2 generated will be diluted by N_2, and the original aim of this process (*i.e.*, CO_2 enrichment and capture) cannot be achieved. The alternative way to integrate CLC with Ca looping is to couple the fuel reactor (FR) with the calciner (provided that the reduction of OC is an exothermic process), so that not only the heat transferred by OC from the AR but also the heat released from the reduction of OC can be utilized in the calciner.

* Corresponding author.
E-mail address: klinsmannzhb@163.com (H. Zhao).

https://doi.org/10.1016/j.cjche.2020.06.033
1004-9541/

Based on the above reasons, a novel Ca—Cu looping process which integrates Cu-based CLC into Ca looping was proposed by Abanades *et al.* [8–10]. A mixture of CaO and CuO with adequate proportions was chosen as cycling medium for facilitating the heat transfer between the two components. In this process, three reactors, carbonator, air reactor and calciner, are interconnected. The carbonation of CaO (Eq. (R1)) happens in the carbonator. Subsequently, the produced $CaCO_3$ and Cu circulate into the air reactor. In the air reactor, Cu is oxidized to generate CuO (Eq. (R2)). The products of the above two reactors, $CaCO_3$ and CuO, are then transported into the calciner, where the reduction of CuO with CH_4 (Eq. (R3)) and calcination of $CaCO_3$ (Eq. (R4)) occur simultaneously. The heat required in Eq. (R4) is provided *in situ* by Eq. (R3).

$$CaO(s) + CO_2 \rightarrow CaCO_3(s) \quad \Delta H_{298K} = -178.8\,kJ \cdot mol^{-1} \tag{R1}$$

$$Cu(s) + 0.5O_2 \rightarrow CuO(s) \quad \Delta H_{298K} = -156.1\,kJ \cdot mol^{-1} \tag{R2}$$

$$4CuO(s) + CH_4 \rightarrow 4Cu(s) + CO_2 + 2H_2O \quad \Delta H_{298K} = -195.3\,kJ \cdot mol^{-1} \tag{R3}$$

$$CaCO_3(s) \rightarrow CaO(s) + CO_2 \quad \Delta H_{298K} = 178.8\,kJ \cdot mol^{-1} \tag{R4}$$

Fernandez *et al.* [6,9,10] further developed a full conceptual design of the Ca—Cu looping process based on Abanades' work and discussed the operating conditions and other limiting factors. This work confirmed the potential of the Ca—Cu looping process as a CO_2 capture technology. Manovic and Anthony [11] demonstrated experimentally that composite pellets containing CaO and CuO were suitable for the Ca—Cu looping process and integrating Ca looping with Cu-based CLC was really possible. Although the composite pellets are feasible for Ca—Cu looping, loss-in-capacity of CaO was found even in short cycles in the experiment. Qin *et al.* [12] believed that the low melting point of CuO probably caused the degradation of CaO and concluded that proper operating conditions were helpful to reduce the negative effect from CuO. In order to enhance the CO_2 capture performance of the CaO/CuO-based pellets, Ridha *et al.* [13] investigated the effect of synthetic method of CaO/CuO particles, and the results showed that the physically mixed pellets exhibited the most favorable performance. Recently, Ma *et al.* [14] reported a core-shell structured CaO—CuO/MgO@Al_2O_3 sorbent synthesized *via* the self-assembly template synthesis method [15]. The CO_2 sorbent performs a quite stable CO_2 uptake capacity of *ca.* 0.08 [g CO_2·(g material)$^{-1}$] in the 30 cyclic tests, and can attain the thermal neutrality *via* providing heat from the exothermic reaction between CuO and CH_4 to the $CaCO_3$ decomposition.

Both the reduction of CuO and decomposition of $CaCO_3$ present in the calciner, so it is important to match the kinetics of the two reactions. However, the reduction of CuO proceeds much faster than the decomposition of $CaCO_3$. Qin *et al.* [16,17] found that the addition of steam into the reducing gas could enhance the reaction rate of $CaCO_3$ decomposition and thus help to match the kinetics of the two reactions. Garcia-Lario *et al.* [18] studied the reduction kinetics of the CuO component in CaO/CuO composite carrier with H_2, CO, and CH_4. The effect of gas mixtures (*i.e.* CO and H_2) on the kinetics was also evaluated, and they concluded that the two gas species showed synergistic effect in promoting the reduction rate of CuO.

With the deepening of research on Ca—Cu looping technology, the comparisons between Ca—Cu looping technology and other CO_2 capture technologies were conducted using many kinds of simulation methods. Using the Aspen Hysys software, Martinez *et al.* [19] made a comparison of two hydrogen generation systems, the Ca—Cu looping (with inherent CO_2 capture) system and CH_4 reforming (with MDEA-based post-combustion CO_2 capture) system. The results demonstrated that the Ca—Cu looping system was approximately 6% and 10% higher than the CH_4 reforming system in terms of hydrogen generation efficiency and carbon capture efficiency, respectively. For CO_2 capture, Ozcan *et al.* [20] evaluated the Ca—Cu looping process in comparison with the Ca looping process, the oxy-combustion process and the ammonia-based adsorption CO_2 capture process by process simulations. Pinch analysis was applied to analyze the CO_2 compression and purification unit as well as the heat exchanger network. They found that Ca—Cu looping has the lowest energy efficiency penalty at the same CO_2 capture efficiency. Recently, a techno-economic analysis of a H_2 production plant using the Ca—Cu looping process was also reported by Riva *et al.* [21].

As can be seen from the literature review above, most of the studies focused on the utilization of Ca—Cu looping technology for post-combustion CO_2 capture with hydrogen or power generation [6,8–10,19,22], as well as the performance and reaction kinetics of CaO/CuO composite carriers and techno-economic analysis [12,13,16–18,21]. Up to date, no work has been reported to study Ca—Cu looping system from the perspective of energy quality (exergy). However, to understand the thermodynamic characteristics of Ca—Cu looping system, to find out the reasons of low efficiency and then to further optimize this system, there is an urgent need to carry out detailed process simulations as well as parameter optimizations and exergy analyses. Based on the exergy analyses, the value, position and type of exergy loss could be determined, which will be helpful to improve the system efficiency and reduce the power dissipation.

Based on Manovic and Anthony [11], three types of Ca—Cu looping systems for post-combustion CO_2 capture were constructed by altering the reactor order [20]: ROUTE 1) carbonation–calcination/reduction–oxidation; ROUTE 2) carbonation–oxidation–calcination/reduction; ROUTE 3) carbonation/oxidation–calcination/reduction. The simplified diagrams of the three different Ca—Cu looping processes are shown in Fig. 1. In this work, process simulations and sensitivity analyses of the three Ca—Cu looping systems (ROUTE 1, ROUTE 2 and ROUTE 3) and a conventional Ca looping system [23,24] (ROUTE 4, as shown in Fig. 1 (d), conducted for comparison) are first conducted using the software Aspen Plus. Based on the simulation results, the exergy analyses are then conducted in detail to find out which route has the best performance.

2. Process Simulations of Four Different ROUTEs

In this study, a typical 600 MW_{th} supercritical pulverized coal fired plant (flue gas with a mass flow rate of 650 kg·s^{-1}, temperature of 40 °C, and at 10^5 Pa) was chosen as the upstream reference plant [25]. As the CO_2 capture unit is set behind the gas purification systems (*i.e.* the desulphurization, denitration, and dedusting systems), the influences of SO_x, NO_x and particulate matters are neglected in the simulations. Compositions of the flue gas from the power generation unit are summarized in Table 1.

In this work, pure CH_4 is used as the reducing gas and the excess ratio of CuO is set to be 30% [20,26] to guarantee the complete combustion of CH_4. In order to ensure the complete oxidation of Cu in the air reactor, air should also be excessive. Therefore, the molar fraction of O_2 at the outlet of the air reactor is fixed to be 3 mol%. Separation efficiencies of the cyclones are assumed to be 100% [27]. In the simulation of Ca looping system, pure CH_4 is used as fuel to supply heat for the decomposition of $CaCO_3$. The molar fraction of O_2 at the calciner outlet is also fixed to be 3 mol%. High-purity O_2 is supplied by a cryogenic air separation unit (ASU) and the molar fraction of O_2 is set to be 98 mol%. The carbonation temperature is set to be 650 °C [27] for both Ca—Cu looping and Ca looping. Although the most researchers set the air reactor to be operated under high pressure (to avoid the decomposition of $CaCO_3$) and high temperature conditions in Ca—Cu looping [6,8], in this work we adopt 1 bar for the air reactor (as well as the other reactors) because of the realizability and operability of the interconnected reactor

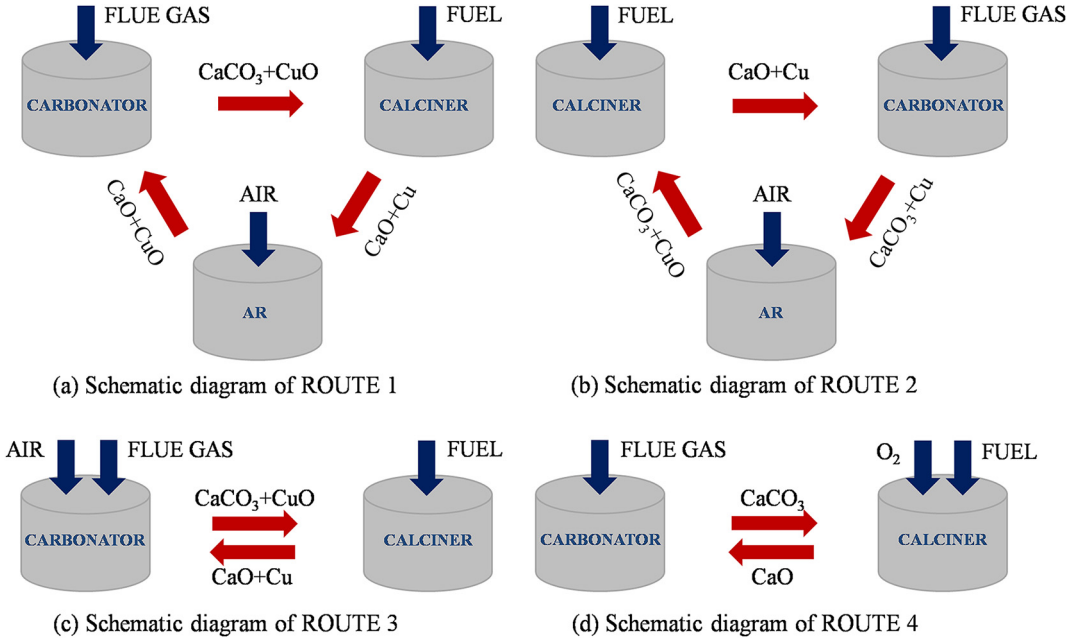

Fig. 1. Schematic diagram of the four Ca—Cu looping ROUTEs studied in the simulation.

systems. According to preliminary thermodynamic and kinetics analysis [3,7,17,25], 650 °C is determined as a suitable temperature condition. The autothermal operation is achieved in the calciners and no external thermal energy input is needed for the three Ca—Cu looping systems.

The determination of the operating parameters is a basis for further analyzing the simulation systems. Therefore, the effects of the operating parameters, such as the temperature of the calciner, the molar flow rates of $CaCO_3$, CH_4 and CuO, and the mass flow rate of air, on the molar fraction of the key component at the carbonator/calciner outlet, the net heat of the calciner and the carbonation conversion efficiency (E_{CO2}) are first studied in this work. E_{CO2} is defined as [28,29],

$$E_{CO2} = \frac{F_{solid} X_{carb}}{F_{CO2}} \quad (1)$$

where F_{solid} represents the molar flow rate of solid particles into the carbonator; X_{carb} is the molar fraction of the CaO in solid particles; F_{CO2} is the molar flow rate of CO_2 contained in the flue gas.

To evaluate the system performance, the ranges of the operating parameters must be given before the formal simulations. According to the previous studies [7,8,12,19], the ranges for the Ca—Cu looping are determined as follows: the temperature of the calciner is 750–950 °C, the molar flow rate of $CaCO_3$ and Cu/Ca ratio are 4000–6000 $kmol \cdot h^{-1}$ and 4.3–7.0, respectively.

2.1. ROUTE 1: carbonation–calcination/reduction–oxidation

Diagram of the material and energy flows in ROUTE 1 is presented in Fig. 2. In this work, the flue gas from the power generation unit firstly enters the carbonator. Before entering the carbonator, the flue gas is pre-heated by the high temperature exhaust gas from the cyclone (SEP1). In the carbonator, the CaO absorbs CO_2 from the flue gas. The high temperature solid stream (CaO + $CaCO_3$ + CuO) separated by SEP1 is then transported into the calciner. In the calciner, calcination of $CaCO_3$ and reduction of CuO occur simultaneously. Then, the solid products, CaO + Cu + CuO, are separated by the cyclone (SEP2), and circulate into the air reactor. Meanwhile, the high temperature gas stream, CO_2 + H_2O, of the SEP2 is used to pre-heat the reducing gas, CH_4. In the air reactor, Cu is oxidized by air to reproduce CuO. The outlet stream of the air reactor is also separated into a solid stream, CaO + CuO, and a gas stream, N_2 + O_2. The solid stream then circulates back to the carbonator for the next cycle, while the gas stream is used to pre-heat the air stream feeding the air reactor.

Table 1
Compositions of the flue gas [25]

Component	CO_2	N_2	H_2O	O_2
Mass fraction/%	12.0	74.2	8.3	5.5

2.2. ROUTE 2: carbonation–oxidation–calcination/reduction

ROUTE 2 is similar with ROUTE 1 in process design except the orders of the carbonator and calciner. The main solid components flowing into the air reactor are $CaCO_3$ and Cu rather than CaO and Cu. Therefore, the operation condition of the air reactor should be carefully determined to make sure that the decomposition of $CaCO_3$ does not take place in this reactor. Garcia-Labiano *et al.* [30] pointed out that Cu can be completely oxidized by air above 500 °C, and the thermodynamic analysis showed that $CaCO_3$ did not decompose at 650 °C, 1 bar. So the temperature of the air reactor is set to be 650 °C. Fig. 3 illustrates the diagram of the material and energy flows in ROUTE 2.

2.3. ROUTE 3: carbonation/oxidation–calcination/reduction

As shown in Fig. 4, the main difference of ROUTE 3 with the above two routes is the absent of the air reactor. The carbonation of CaO and oxidization of Cu occur simultaneously in the carbonator, and the reduction of CuO with CH_4 and calcination of $CaCO_3$ occur simultaneously in the calciner. The high temperature exhaust gas of the carbonator is used to preheat the mixtures of flue gas and air, while the exhaust gas of the calciner is used to preheat the fuel, CH_4.

2.4. ROUTE 4: Ca looping

Different from Ca—Cu looping, the heat required in calcination of $CaCO_3$ is provided by the oxy-combustion of CH_4 in Ca looping. The high-purity O_2 required is generated by an air separation unit (ASU)

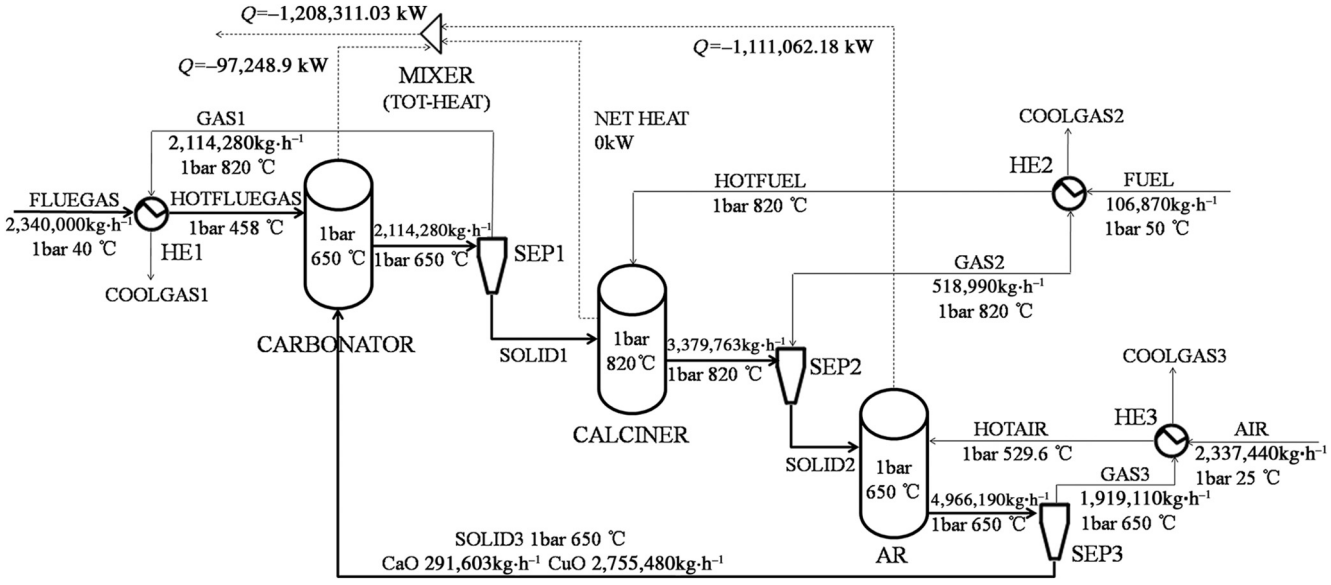

Fig. 2. Diagram of the material and energy flows in ROUTE 1 (1 bar=10^5 Pa).

which consists of a multistage compressor, a heat exchanger, a distillation column and a throttle valve. From the flow sheet of the Ca looping (Fig. 5), it can be seen that the flue gas is preheated by the outlet gas stream of carbonator and then reacts with CaO in the carbonator. The combustion of CH_4 in the calciner is used to provide heat to the calcination of $CaCO_3$. And then the high temperature exhaust gas of the calciner is divided into two parts by a splitter: one part is used to preheat the fuel and another is used to preheat the oxygen.

2.5. Sensitivity analysis

2.5.1. Influence of the calcination temperature

The effects of the calcination temperature on the mole fractions of CO_2 and CaO at the calciner outlet are shown in Fig. 6. As can be seen, in the three Ca—Cu looping routes, the mole fractions of CO_2 and CaO increase with the calcination temperature before 820 °C and over this point, the calcination temperature has little influence on the system's performance. The same trend is also observed in ROUTE 4, but the turning point changes to 840 °C. As a consequence, the optimal calcination temperature is determined to be 820 °C for ROUTEs 1, 2 and 3, and 840 °C for ROUTE 4.

In Fig. 6, the CO_2 volume fraction in the three Ca—Cu looping routes is higher than that in the Ca looping before 780 °C, which is due to the reduction of CuO (Eq. (R3)) in the Ca—Cu looping. The calcination of $CaCO_3$ occurs rapidly above 780 °C and with the increase of temperature the calcination process can proceed more completely because the reaction equilibrium will shift to the right side at high temperatures. The optimal calcination temperature of Ca looping (840 °C) is higher than that

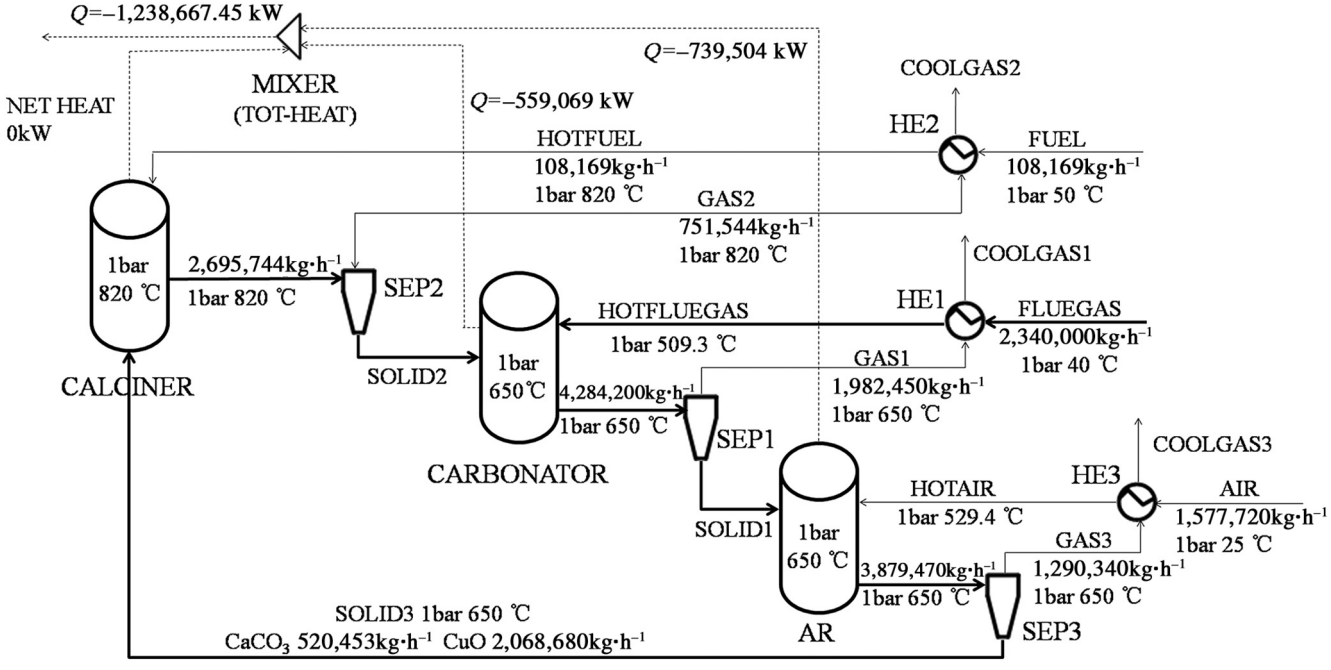

Fig. 3. Diagram of the material and energy flows in ROUTE 2.

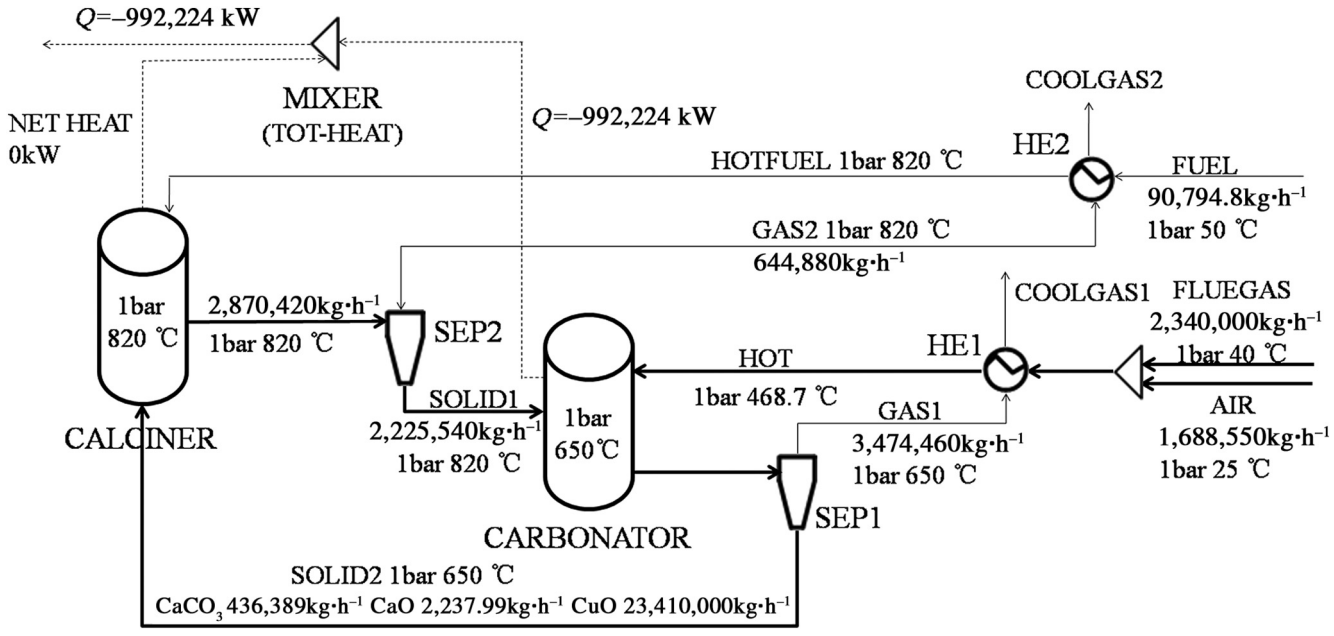

Fig. 4. Diagram of the material and energy flows in ROUTE 3.

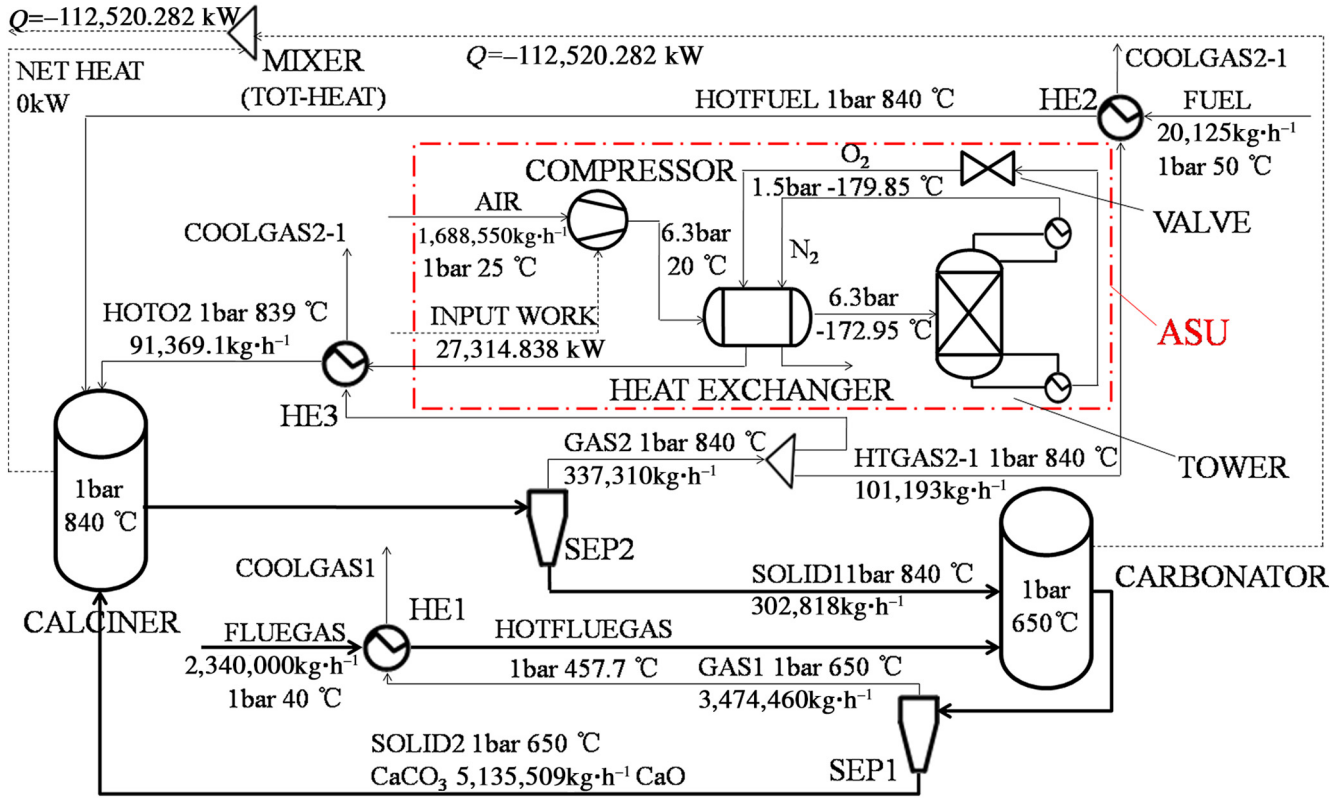

Fig. 5. Diagram of the material and energy flows in ROUTE 4.

of Ca—Cu looping (820 °C). This may be due to the influence of Cu components on the calcination reaction.

2.5.2. Influence of the molar flow rate of $CaCO_3$

Fig. 7 shows the influences of the molar flow rate of $CaCO_3$ on the mole fraction of CO_2 at the carbonator outlet and the conversion efficiency of CO_2 (E_{CO2}) in the carbonator. Before reaching the inflection point, the mole fraction of CO_2 decreases and E_{CO2} increases as the molar flow rate of $CaCO_3$ increases. This is mainly because that with the increasing of molar flow rate of $CaCO_3$, the molar flow rate of the generated CaO increases, thus more CO_2 in the flue gas is absorbed. After the inflection point, the mole fraction of CO_2 and E_{CO2} become insensitive to the molar flow rate of $CaCO_3$. The inflection points of the four routes are not strictly identical, and the smallest value is found in

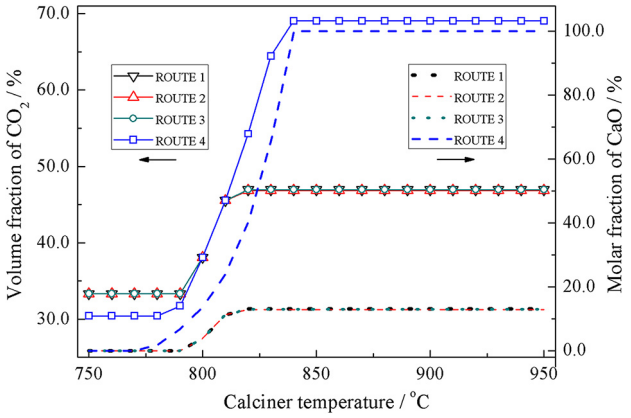

Fig. 6. Influence of the calcination temperature on the mole fractions of CO_2 and CaO at the calciner outlet.

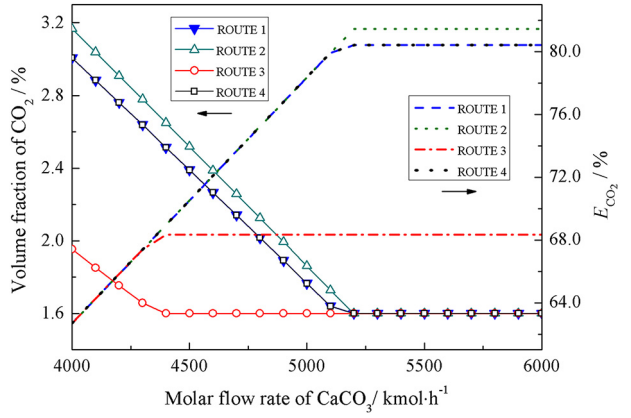

Fig. 7. Influence of molar flow rate of $CaCO_3$ on the carbonator performance.

ROUTE 3, which suggests that ROUTE 3 has worst adsorption capacity. This is because the CO_2 in the flue gas is diluted by a large amount of air entering into carbonator in ROUTE 3, and the carbonation conversion decreases with the decreases of CO_2 concentration. The optimal molar flow rate of $CaCO_3$ is determined to be 5200 kmol·h^{-1} for ROUTEs 1, 2 and 4, and 4400 kmol·h^{-1} for ROUTE 3.

2.5.3. Influence of the Cu/Ca ratio

The influence of Cu/Ca ratio is only investigated for the Ca—Cu looping systems. As shown in Fig. 8, the mole fractions of CO_2 and H_2O at the calciner outlet increase with the increasing of Cu/Ca ratio initially and then the values remain unchanged after reaching the inflection points. This is because the decomposition of $CaCO_3$ and reduction of CuO release more CO_2 and H_2O under the higher Cu/Ca ratio condition. The net heat of the calciner (Q) decreases initially and then increases with the Cu/Ca ratio. If Q is equal to zero, the neutrally thermal condition in the calcination–reduction step is archived. As for the three routes, different process configurations result in different stream temperatures entering the calciner, which makes the Cu/Ca ratios different to achieve the auto-thermal balance. Here, the optimal Cu/Ca ratios are determined to be 5.13, 5.19, and 5.16 for ROUTEs 1, 2, and 3, respectively.

2.6. Analysis of the simulation results

According to the above analyses, the optimal operation conditions of the four routes are listed in Table 2.

As shown in Table 2, the flow rate of air is of the following decreasing order: ROUTE 1, ROUTE 3, ROUTE 2 and ROUTE 4. The flow rate of air in ROUTE 1 is the largest, because of the high molar flow rate of CuO and no use of O_2 in the flue gas (the feeding material of the carbonator is CuO rather than Cu). In ROUTEs 2 and 3, the O_2 in the flue gas can be used because Cu is fed into the carbonator in these routes. The molar flow rate of air in ROUTE 2 is expected larger than that in ROUTE 3 because the molar flow rate of CuO in ROUTE 2 is larger than that in ROUTE 3. However, the setting of the excess O_2 ratio at the reactor outlet increases the oxygen demand of ROUTE 3. The minimum air flow rate is attained in ROUTE 4, mainly because air has a different role in this system. In Ca—Cu looping, the heat required in the calciner is provided by the reduction of CuO with CH_4, while in Ca looping, the heat required in the calciner is provided by the oxy-combustion of CH_4. Due to the fact that the oxy-combustion of CH_4 can release more heat than the reduction of CuO with CH_4, the molar flow rates of air and CH_4 in Ca looping are smaller than that in Ca—Cu looping.

Table 3 shows the main results of the simulations. It can be seen that the same "CuO conversion" was obtained for the three Ca—Cu routes, because all the excess ratios of CuO in the three routes are set to be 30%. In the simulations, the thermal neutrality ($Q = 0$ kW) of the calciners is ensured to reach by setting the "design spec", and the excessive air is introduced into the air reactor to make sure that Cu could be fully converted.

The "carbonation conversion" and the "$CaCO_3$ conversion" correspond to the absorption of CO_2 in the carbonator and desorption of CO_2 in the calciner, respectively. It can be seen from Table 3 that the decomposition of $CaCO_3$ can proceed completely in the four routes; ROUTE 2 has the highest carbonation conversion while ROUTE 3 has the lowest, it is because in ROUTE 2 the high CO_2 concentration in the flue gas caused by the consumption of O_2 facilitates the carbonation conversion; on the other side, although the O_2 in the flue gas is also consumed by Cu partial oxidation in ROUTE 3, the CO_2 concentration decreases as a large amount of N_2 is introduced into the carbonator; the same carbonation conversion efficiency is obtained in ROUTE 1 and in ROUTE 4 because of the same CO_2 concentration, operation temperature and pressure of the carbonators.

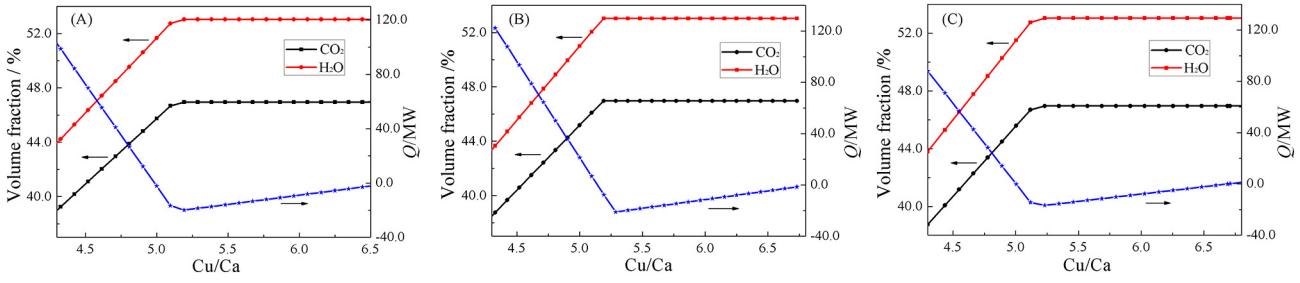

Fig. 8. Influence of Cu/Ca ratio on calciner performance in (a) ROUTE 1, (b) ROUTE 2 and (c) ROUTE 3.

Table 2
Optimal operation conditions of the four routes

	Calciner temperature/°C	$CaCO_3$ flow rate/kmol·h^{-1}	Cu/Ca molar ratio	Air flow rate/kg·h^{-1}	CH_4 flow rate/kmol·h^{-1}	CuO flow rate/kmol·h^{-1}
ROUTE 1	820	5200	5.13	2.33744×10^6	6661.59	34,640.30
ROUTE 2	820	5200	5.19	1.66267×10^6	6742.51	35,061.00
ROUTE 3	820	4400	5.16	1.68855×10^6	5659.55	29,429.70
ROUTE 4	840	5200	/	4.83406×10^5	1324.61	/

Table 3
Main results of the simulations

		Carbonator	Calciner		Air reactor
	Net heat of calciner/kW	Carbonation conversion/%	$CaCO_3$ conversion/%	CuO conversion/%	Cu conversion/%
ROUTE 1	0	80.41	100	76.92	100
ROUTE 2	0	81.44	100	76.92	100
ROUTE 3	0	68.33	100	76.92	100
ROUTE 4	0	80.41	100		

3. Exergy Analysis

The kinetic exergy and potential exergy of the stream are so small that they are neglected in the exergy calculations, and only the physical exergy and chemical exergy are included. The method to calculate the physical and chemical exergy is the same as that in Xiong *et al.* [31].

The exergy destruction (E_D) is mainly used to express the exergy depletion due to the irreversibility in a system or units, while the exergy loss (E_L) is usually used to represent the leakage of exergy into the environment and/or the emission of exergy within the by-products. Analyses results are shown in Figs. 9–12.

The exergy efficiency (η, Eq. (2)) [31] is introduced here to identify the performance of the four routes from the viewpoint of thermodynamic. The exergy destruction ratio (y_D, Eq. (3)) [31] and exergy destruction distribution (ε, Eq. (4)) [31] are also calculated. y_D means the ratio of the exergy destruction in one unit to the total exergy of fuel (E_F), and ε is the ratio of the exergy destruction in one unit to the total exergy destruction in the system. These parameters are defined as:

$$\eta = \frac{E_P}{E_F} = 1 - \frac{(E_D + E_L)}{E_F} \tag{2}$$

$$y_D = \frac{E_D}{E_{F,tot}} \tag{3}$$

$$\varepsilon = \frac{E_D}{E_{D,tot}} \tag{4}$$

where, E_F, E_P, E_D and E_L represent the fuel exergy, the product exergy, the exergy destruction and the exergy loss, respectively. "Fuel" in the simulations includes CH_4 and air. CO_2 is defined as the "product". The exergy carried by streams of COOLGAS1 and COOLGAS3 is defined as the exergy loss.

It can be found from Fig. 9(a) that in ROUTE 1 the exergy destruction of the calciner is the largest (53.51%), which indicates that the exergy destruction is mainly caused by chemical reactions. The sum of the exergy destructions in the heat exchangers (*i.e.* HE1, HE2, and HE3) reaches to 16.51% and the largest one is found in HE1 because this heat exchanger has the largest heat transfer temperature difference. As shown in Fig. 9(b), for ROUTE 1, the exergy loss and exergy efficiency of the system are 2.64% and 62.81%, respectively.

As shown in Fig. 10(a), the calciner is also the main exergy destruction unit in ROUTE 2, but the proportion is changed to 55.37%. Compared with ROUTE 1, the proportion of the exergy destruction increases in the carbonator while decreases in the air reactor. This is because part of Cu is oxidized by O_2 in the flue gas in the carbonator; the amount of Cu oxidized in the air reactor thus decreases. Fig. 10 (b) shows that for ROUTE 2, the exergy loss and exergy efficiency of the system are 1.86% and 65.04%, respectively.

The only difference between ROUTE 1 and ROUTE 2 is the order of the reactors, while the exergy efficiency of ROUTE 2 is higher than that of ROUTE 1. This can be understood from the aspects of exergy loss and exergy destruction. The exergy of COOLGAS1 in ROUTE 1 is larger than that in ROUTE 2 because the O_2 in the flue gas cannot be used in ROUTE 1. The exergy of COOLGAS3 in ROUTE 1 is also larger than that in ROUTE 2, which is mainly because the amount of air flowing into the air reactor in ROUTE 1 is larger than that in ROUTE 2. As the exergy of the COOLGAS1 and COOLGAS3 is defined as the exergy loss, the exergy loss in ROUTE 1 is larger than that in ROUTE 2. As for the exergy destruction, it can be found that the main difference lies in the air reactor, and the exergy destruction in the air reactor in ROUTE 1 is larger than that of in ROUTE 2.

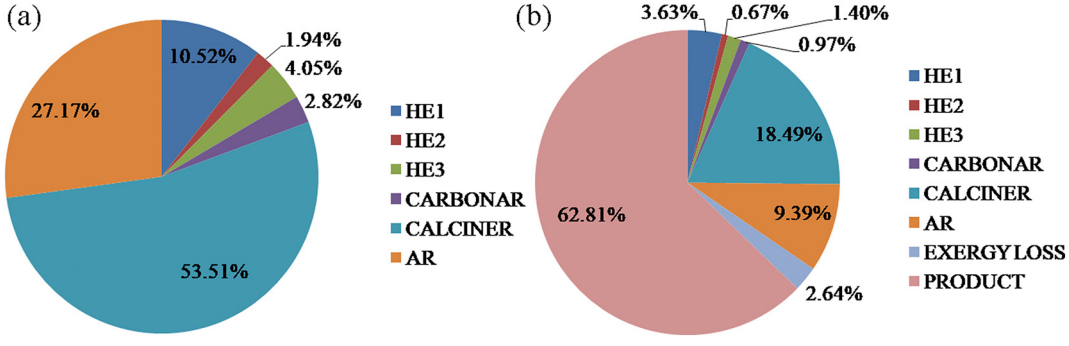

Fig. 9. The (a) exergy destruction distribution and (b) exergy destruction ratio in ROUTE 1.

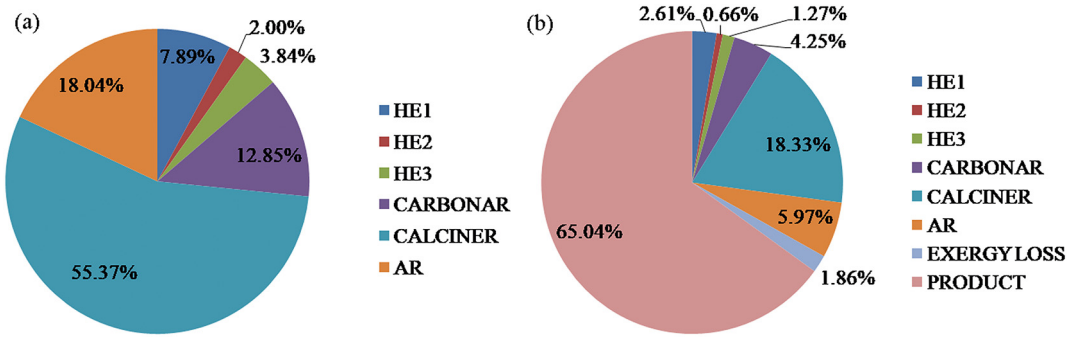

Fig. 10. The (a) exergy destruction distribution and (b) exergy destruction ratio in ROUTE 2.

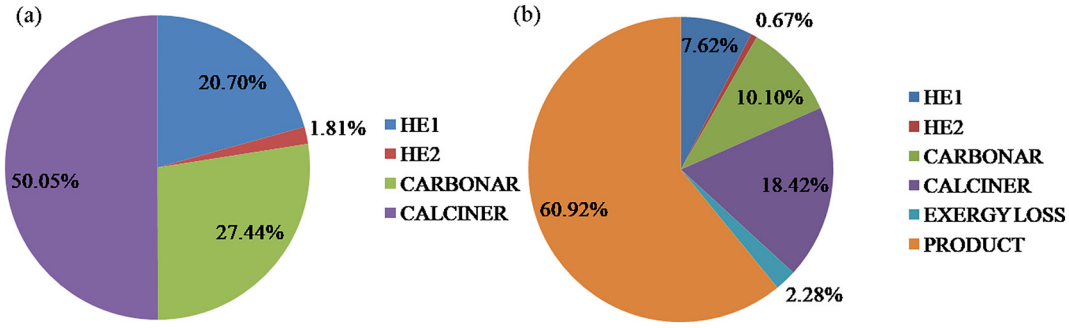

Fig. 11. The (a) exergy destruction distribution and (b) exergy destruction ratio in ROUTE 3.

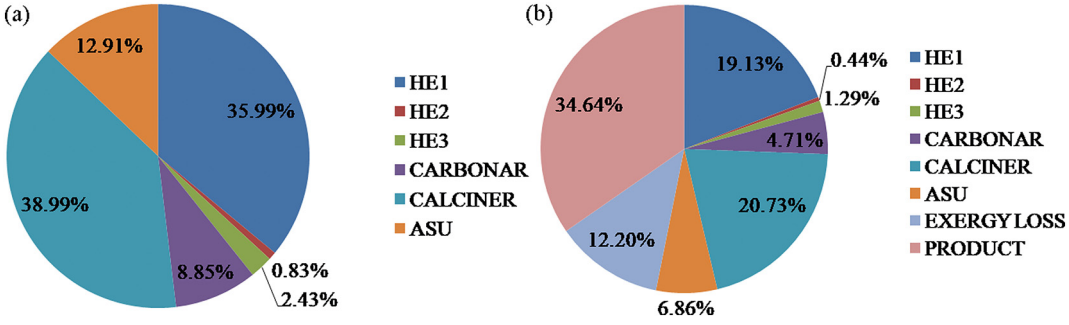

Fig. 12. The (a) exergy destruction distribution and (b) exergy destruction ratio in ROUTE 4.

Because the exergy destruction is mainly caused by chemical reactions, the more reactions happen, the more exergy destruction obtains. Both the oxidation and carbonation reactions happen in the carbonator simultaneously in ROUTE 3, the exergy destruction in ROUTE 3 is larger than that in ROUTEs 1 and 2. According to Fig. 11(b), the exergy loss of the system is 2.28% and the exergy efficiency is 60.92% for ROUTE 3.

In ROUTE 4, only the chemical reactions of carbonation and calcination happen, and the oxidation and reduction reactions are absent. Thus the exergy destruction in ROUTE 4 is less than that in the former three Ca—Cu routes. However, the exergy destruction caused by the additional air separation unit (ASU) is considerably high. As shown in Fig. 12(b), the exergy loss of the system is 12.20% and the exergy efficiency is only 34.64% for ROUTE 4.

4. Conclusions

Autothermal balance cannot be achieved in the conventional Ca looping for post-combustion CO_2 capture, thus an air separation unit is needed. In Ca—Cu looping, not only the autothermal balance can be achieved, but also the direct contact between fuels and air can be avoided. In this work, the processes of Ca—Cu looping for post-combustion CO_2 capture are designed to assess the Ca—Cu looping from the viewpoints of thermodynamics and to compare with the conventional Ca looping. The results of the sensitivity analyses show that three Ca—Cu routes have nearly the same key operation parameters and the calcination temperature needed for Ca looping is slightly higher than that of Ca—Cu looping. The optimal Cu/Ca ratio for Ca—Cu looping is in the range of 5.13–5.19. Due to the largest CO_2 concentration in carbonator, ROUTE 2 is found to have the highest CO_2 capture efficiency, up to 81.44%. ROUTE 2 has the highest exergy efficiency, which is up to 65.04% and is about 30% larger than that of Ca looping. ROUTE 3 has the lowest exergy efficiency among the three Ca—Cu routes because of the lowest carbonation conversion caused by the lowest CO_2 concentration. In the four routes, the exergy destruction mainly happens in the reactors, especially in the calciner. Since the exergy destruction in the heat exchangers is also considerably high, further studies on the design of

heat exchange network are still required to enhance the exergy efficiency of the four routes. Furthermore, the results obtained here are based on process simulations, thus further experimental validations are still needed.

Acknowledgements

This work was financially supported by National Key R&D Program of China (2019YFE0100100).

References

[1] H. Zhao, X. Tian, J. Ma, X. Chen, M. Su, C. Zheng, Y. Wang, Chemical looping combustion of coal in China: comprehensive progress, remaining challenges, and potential opportunities, *Energ Fuel.* 34 (6) (2020) 6696–6743.
[2] J. Blamey, E.J. Anthony, J. Wang, P.S. Fennell, The calcium looping cycle for large-scale CO_2 capture, *Prog. Energ. Combust.* 36 (2010) 260–279.
[3] L. Duan, T. Feng, S. Jia, X. Yu, Study on the performance of coal-fired power plant integrated with Ca-looping CO_2 capture system with recarbonation process, *Energy.* 115 (2016) 942–953.
[4] V. Dupont, A.B. Ross, E. Knight, I. Hanley, M.V. Twigg, Production of hydrogen by unmixed steam reforming of methane, *Chem. Eng. Sci.* 63 (2008) 2966–2979.
[5] T. Shimizu, T. Hirama, H. Hosoda, K. Kitano, M. Inagaki, K. Tejima, A twin fluid-bed reactor for removal of CO_2 from combustion processes, *Chem. Eng. Res. Des.* 77 (1999) 62–68.
[6] J.R. Fernández, J.C. Abanades, R. Murillo, G. Grasa, Conceptual design of a hydrogen production process from natural gas with CO_2 capture using a Ca-Cu chemical loop, *Int. J. Greenh. Gas. Con.* 6 (2012) 126–141.
[7] I. Martínez, J.R. Fernández, J.C. Abanades, M.C. Romano, Integration of a fluidised bed Ca–Cu chemical looping process in a steel mill, *Energy.* 163 (2018) 570–584.
[8] J.C. Abanades, R. Murillo, J.R. Fernandez, G. Grasa, I. Martínez, New CO_2 capture process for hydrogen production combining Ca and Cu chemical loops, *Environ. Sci. Technol.* 44 (2010) 6901–6904.
[9] I. Martínez, J.R. Fernández, G. Grasa, Ca-Cu chemical looping process for hydrogen and/or power production, In: Global Warming and Climate Change, *IntechOpen* (2018)https://doi.org/10.5772/intechopen.80855.
[10] I. Martínez, J.R. Fernández, M. Martini, F. Gallucci, M.Van.Sint. Annaland, M.C. Romano, J.C. Abanades, Recent progress of the Ca-Cu technology for decarbonisation of power plants and carbon intensive industries, *Int. J. Greenh. Gas. Con.* 85 (2019) 71–85.
[11] V. Manovic, E.J. Anthony, Integration of calcium and chemical looping combustion using composite CaO/CuO-based materials, *Environ. Sci. Technol.* 45 (2011) 10750–10756.
[12] C. Qin, J. Yin, W. Liu, H. An, B. Feng, Behavior of CaO/CuO based composite in a combined calcium and copper chemical looping process, *Ind. Eng. Chem. Res.* 51 (2012) 12274–12281.
[13] F.N. Ridha, D. Lu, A. Macchi, R.W. Hughes, Combined calcium looping and chemical looping combustion cycles with CaO-CuO pellets in a fixed bed reactor, *Fuel.* 153 (2015) 202–209.
[14] J. Ma, D. Mei, W. Peng, X. Tian, D. Ren, H. Zhao, On the high performance of a core-shell structured CaO-CuO/MgO@Al_2O_3 material in calcium looping integrated with chemical looping combustion (CaL-CLC), *Chem. Eng. J.* 368 (2019) 504–512.
[15] H. Zhao, X. Tian, J. Ma, M. Su, B. Wang, D. Mei, Development of tailor-made oxygen carriers and reactors for chemical looping processes at Huazhong University of Science & Technology, *Int. J. Greenh. Gas. Con.* 93 (2020) 102898.
[16] C. Qin, J. Yin, C. Luo, H. An, W. Liu, B. Feng, Enhancing the performance of CaO/CuO based composite for CO_2 capture in a combined Ca-Cu chemical looping process, *Chem. Eng. J.* 228 (2013) 75–86.
[17] C. Qin, B. Feng, J. Yin, J. Ran, L. Zhang, V. Manovic, Matching of kinetics of $CaCO_3$ decomposition and CuO reduction with CH_4 in Ca-Cu chemical looping, *Chem. Eng. J.* 262 (2015) 665–675.
[18] A.L. Garcia-Lario, I. Martinez, R. Murillo, G. Grasa, J.R. Fernandez, J.C. Abanades, Reduction kinetics of a high load Cu-based pellet suitable for Ca/Cu chemical loops, *Ind. Eng. Chem. Res.* 52 (2013) 1481–1490.
[19] I. Martinez, M.C. Romano, J.R. Fernandez, P. Chiesa, R. Murillo, J.C. Abanades, Process design of a hydrogen production plant from natural gas with CO_2 capture based on a novel Ca/Cu chemical loop, *Appl. Energ.* 114 (2014) 192–208.
[20] D.C. Ozcan, A. Macchi, D. Lu, A.M. Kierzkowska, H. Ahn, C.R. Muller, S. Brandani, Ca-Cu looping process for CO_2 capture from a power plant and its comparison with Ca-looping, oxy-combustion and amine-based CO_2 capture processes, *Int. J. Greenh. Gas. Con.* 43 (2015) 198–212.
[21] L. Riva, I. Martínez, M. Martini, F. Gallucci, M.V.S. Annaland, M.C. Romano, Techno-economic analysis of the Ca-Cu process integrated in hydrogen plants with CO_2 capture, *Int. J. Hydrogen. Energ.* 43 (2018) 15720–15738.
[22] I. Martinez, R. Murillo, G. Grasa, J.R. Fernandez, J.C. Abanades, Design of a hydrogen production process for power generation based on a Ca-Cu chemical loop, *Energy Procedia* 37 (2013) 626–634.
[23] I. Martinez, G. Grasa, R. Murillo, B. Arias, J.C. Abanades, Modelling the continuous calcination of $CaCO_3$ in a Ca-looping system, *Chem. Eng. J.* 215 (2013) 174–181.
[24] J.C. Abanades, The maximum capture efficiency of CO_2 using a carbonation/calcination cycle of CaO/$CaCO_3$, *Chem. Eng. J.* 90 (2002) 303–306.
[25] H. Chen, Z. Wang, W. Wu, J. Tong, Process simulation of the multiple cyclic CCRs system for CO_2 capture based on Aspen Plus, *J. Chin. Soc. Power Eng.* 32 (2012) 558–561.
[26] C.R. Forero, P. Gayan, F. Garcia-Labiano, L.F. De Diego, A. Abad, J. Adanez, High temperature behaviour of a CuO/γ-Al_2O_3 oxygen carrier for chemical-looping combustion, *Int. J. Greenh. Gas. Con.* 5 (2011) 659–667.
[27] A. Lasheras, J. Strohle, A. Galloy, B. Epple, Carbonate looping process simulation using a 1D fluidized bed model for the carbonator, *Int. J. Greenh. Gas. Con.* 5 (2011) 686–693.
[28] C. Hawthorne, M. Trossmann, P.G. Cifre, A. Schuster, G. Scheffknecht, Simulation of the carbonate looping power cycle, *Energy Procedia* 1 (2009) 1387–1394.
[29] A. Charitos, C. Hawthorne, A.R. Bidwe, H. Spliethoff, G. Scheffknecht, Parametric investigation of the calcium looping process for CO_2 capture in a 10 kW_{th} dual fluidized bed, *Int. J. Greenh. Gas. Con.* 4 (2010) 776–784.
[30] F. Garcia-Labiano, L.F. De Diego, J. Adanez, A. Abad, P. Gayan, Reduction and oxidation kinetics of a copper-based oxygen carrier prepared by impregnation for chemical-looping combustion, *Ind. Eng. Chem. Res.* 43 (2004) 8168–8177.
[31] J. Xiong, H. Zhao, C.G. Zheng, Exergy analysis of a 600 MW_e oxy-combustion pulverized-coal-fired power plant, *Energ Fuel.* 25 (2011) 3854–3864.